LBL-24011
Preprint

Lawrence Berkeley Laboratory
UNIVERSITY OF CALIFORNIA

Materials & Chemical Sciences Division

Submitted to Journal of Physical Chemistry

The Molecular Structure of Benzene Coadsorbed with CO on Pd(111): A Dynamical LEED Analysis

H. Ohtani, M.A. Van Hove, and G.A. Somorjai

February 1988

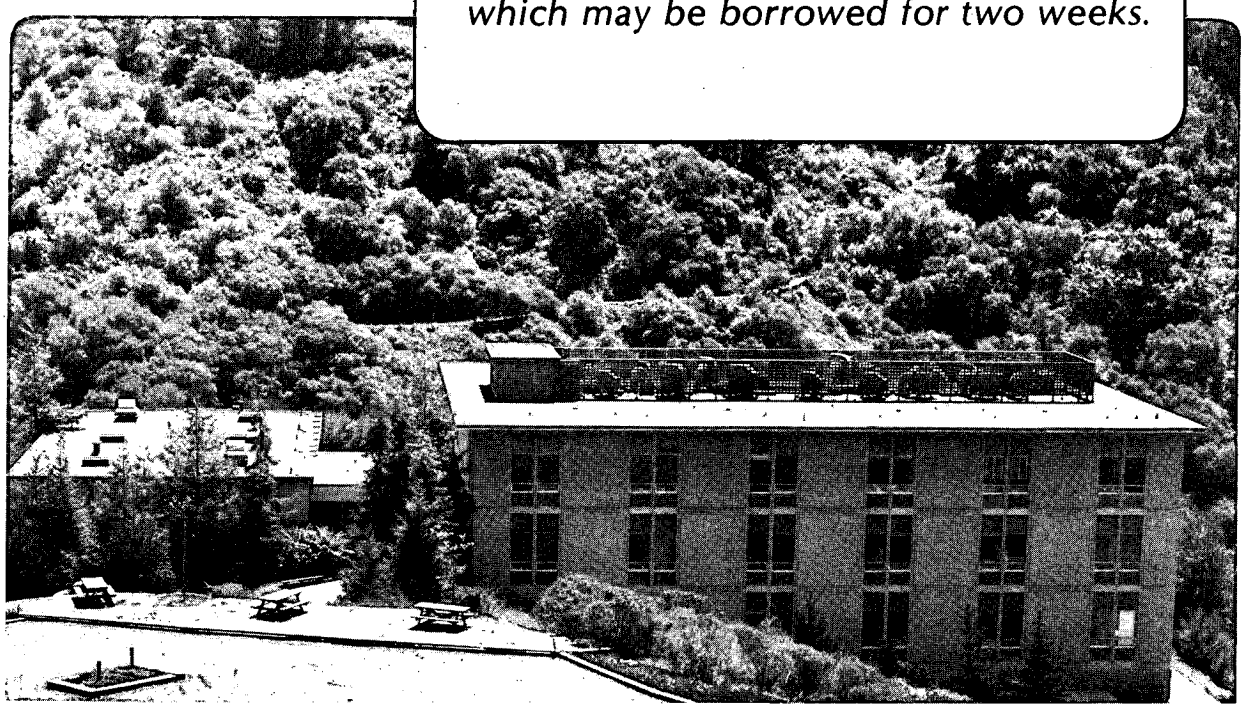

Prepared for the U.S. Department of Energy under Contract DE-AC03-76SF00098

DISCLAIMER

LBL-24011

The Molecular Structure of Benzene Coadsorbed with CO on Pd(111): A Dynamical LEED Analysis

H. Ohtani, M. A. Van Hove, and G. A. Somorjai*

Materials and Chemical Sciences Division, Lawrence Berkeley Laboratory
and Department of Chemistry, University of California, Berkeley, CA 94720

ABSTRACT

The molecular structure of the ordered (3x3) superlattice of coadsorbed C_6H_6 and CO on the Pd(111) crystal face is analyzed by dynamical calculations of low-energy electron diffraction (LEED) intensities.

The benzene molecules are found to be oriented with their carbon rings parallel to the surface, centered over fcc-type 3-fold hollow sites. The C-C bond lengths in the benzene ring skeleton are found to be either 1.40±0.10Å or 1.46±0.10Å depending on the position of the C-C bonds relative to the underlying Pd atoms. These bond lengths are very close to the corresponding gas phase value of 1.397Å. This contrasts with similar coadsorbate systems of benzene and CO on Rh(111) or Pt(111), where significant in-plane distortions and enlargements of the benzene rings have been detected. A trend toward more distortion and increasing average C-C bond length have been found in changing substrates from Pd to Rh and Pt, while the metal-carbon bond lengths decrease in that same

sequence. This is interpreted to indicate that the metal-carbon bond becomes stronger, while C-C bonds weaken from Pd to Rh and Pt, which is further supported by HREELS data.

Coadsorbed CO molecules are necessary to form an ordered benzene overlayer on Pd(111). They occupy fcc-hollow sites surrounding the benzene molecules. The C-O axis is perpendicular to the surface, and the carbon-oxygen and palladium-carbon bond lengths are found to be 1.17±0.05Å and 2.05±0.04Å, respectively.

1. Introduction

In recent years detailed structural information of molecular adsorbates on metal surfaces has been accumulating[1]. Most of these studies use dynamical LEED analysis to determine the structures of rather small molecular adsorbates like CO, C_2H_2, and C_2H_3 (ethylidyne). With the Beam Set Neglect approximation of dynamical LEED analysis, more complex molecular overlayer structures with any size of unit cells could be determined[2]. Using this scheme, three structures of benzene coadsorbed with CO on Pt(111)[3] and Rh(111)[4,5] were analyzed, all of which have rather large unit cells. These systems may be labeled:

I. Pt(111)-$(2\sqrt{3}\times4)$*rect*-$2C_6H_6 + 4CO$

II. Rh(111)-c$(2\sqrt{3}\times4)$*rect*-$C_6H_6 + CO$

III. Rh(111)-(3x3)-$C_6H_6 + 2CO$

In these cases, CO was necessary as the background gas to induce the formation

of stable ordered superlattices of benzene and CO[6]. (Benzene alone forms only a disordered overlayer on Pt(111). On Rh(111) a $(2\sqrt{3}x3)rect\text{-}2C_6H_6$ ordered superstructure can be formed, but this structure is unstable under electron-beam irradiation and also easily contaminated by background CO gas to transform into the coadsorbed superstructures mentioned above.) These structure analyses[3,4,5] have confirmed that the benzene molecules are associatively adsorbed parallel to the surface. Furthermore, in all cases, significant C_6 ring expansions have been revealed compared to the gas phase benzene structure, as well as C-C bonds of unequal lengths within each C_6 ring skeleton. These results prompted us to study the structure of benzene on a third metal, Pd(111), which has the unique property to catalyze acetylene trimerization to form benzene[7–14].

The adsorption properties of benzene on Pd(111) have been extensively studied with various surface science techniques, including Angle Resolved Ultraviolet Photoelectron Spectroscopy (ARUPS)[15,16], Angle Integrated Ultraviolet Photoemission Spectroscopy (UPS)[7], Metastable Noble Gas Deexcitation Spectroscopy (MDS)[7], Thermal Desorption Spectroscopy (TDS)[7,8,10,13,14], Electron Energy Loss Spectroscopy (EELS)[16], and High Resolution Electron Energy Loss Spectroscopy (HREELS)[12,17,18,19]. These studies have indicated that benzene molecules are adsorbed parallel to the Pd(111) surface, bonding through the π electrons at room temperature, like benzene on many other transition metals. HREELS showed an increase of the γ_{CH} out-of-plane bending frequency of adsorbed benzene on Pd(111) surface from the gas phase value. This shift is, however, much smaller than on Rh(111)[20], or Pt(111)[21], indicating that the structure of benzene on

Pd(111) is closer to the gas phase structure, perhaps due to a weaker benzene-Pd(111) interaction. The ARUPS[16] data suggest that the benzene-Pd(111) complex has C_{6v} symmetry although no bond length information has been obtained.

The conversion of acetylene to benzene can proceed under UHV conditions as well as under high-pressure conditions on palladium single-crystal surfaces. This reaction is structure sensitive. The Pd(111) surface is effective under UHV conditions, while both the Pd(111) and Pd(100) are most effective under high pressure conditions[13]. Our structural LEED work on the benzene/Pd(111) system aims at understanding this reaction at a molecular level.

Ordering of the surface structure facilitates the LEED structure analysis. But at no coverage near or above room temperature could we produce an ordered superstructure of pure benzene on Pd(111). In analogy with the situation on Rh(111) and Pt(111), we coadsorbed CO and obtained one well-ordered superlattice, as described in more detail in the next section. The LEED analysis confirmed a parallel adsorption geometry of benzene centered over 3-fold fcc-type hollow site of Pd(111), with little distortion of the C_6 ring. The benzene molecules are interspersed with CO standing perpendicularly to the surface at 3-fold fcc-type hollow sites.

2. Experiment

2.1. Equipment

Experiments were performed in an ion-pumped, stainless steel UHV system, equipped with a quadrupole mass spectrometer, an ion bombardment gun and a four-grid LEED optics. An off-axis electron gun, and the LEED optics were used for Auger electron spectroscopy. We used a palladium crystal of dimensions, 6mm x 8 mm x 0.45 mm, spot-welded to tantalum support wires. The crystal could be cooled to $\sim$ 120 K by conduction from a pair of liquid nitrogen cold fingers or heated resistively to $\sim$ 1500 K. Temperatures were measured by a 0.005" chromel-alumel thermocouple spot-welded to one edge of the palladium crystal. The system base pressure was in the low 10^{-10} torr range. H_2 and CO were the main components of the residual gas.

The LEED optics and vacuum chamber were enclosed by two sets of Helmholtz coils to minimize the magnetic field near the crystal. These coils were adjusted until there was no significant deflection of the specularly-reflected beam over the 20 to 200 eV energy range used for LEED intensity vs. energy (I-V) measurements. There were no exposed insulators or ungrounded conductors in the vicinity of the crystal in order to minimize electrostatic fields. The LEED electron gun was operated in the space-charge limited mode, so that the beam current increased monotonically and approximately linearly over the voltage range used. At 200 eV the beam current was $\sim 4.0\mu$-amps. The intensity-energy curves were normalized with respect to incident beam current. The crystal was mounted on a manipulator capable of independent azimuthal and co-latitude rotations. The crystal surface was oriented with the (111) face perpendicular to

the azimuthal rotation axis as determined by visual comparison of the intensities of symmetry related substrate beams. It is possible to see deviations from normal incidence of less than 0.2° with this method. The accuracy of the orientation was confirmed by the close agreement of I-V curves for symmetry-related beams. The off-normal incidence angles were set by rotating the crystal away from the experimentally determined normal-incidence position using a scale inscribed on the manipulator.

LEED data were collected using a high-sensitivity vidicon TV camera with a f/.85 lens. The data were recorded on video tapes, and the diffraction patterns were analyzed using a real-time video digitizer interfaced to an LSI-11 microcomputer[22]. Twenty consecutive video frames at constant energy were summed to improve the signal/noise ratio, and an image recorded at zero beam voltage was subtracted to correct for the camera dark current and stray light from the LEED screen or filament. After such analysis at each energy, I-V curves were generated by a data reduction program that locates diffraction spots in the digitized image, integrates the spot intensity, and makes local background corrections[23].

2.2. Sample Preparation

The major impurities in the Pd(111) crystals were sulfur and carbon. These were removed by several cycles of oxidation ($P_{O_2} = 5\text{x}10^{-7}$torr, 400C) and 500 eV argon ion bombardment ($P_{Ar} = 5\text{x}10^{-5}$torr, both at room temperature and at 600C) followed by annealing at 500C. Right before the experiment, the crystal was flashed to 600C to desorb adsorbed CO and H originating from the

background gas in the UHV chamber and to remove any residual carbon by diffusion into the bulk[24]. The surface cleanliness was checked by AES. The clean Pd(111) surface showed a sharp (1x1) LEED pattern with very low background intensity. The surface structure of clean Pd(111) surface prepared by this method was confirmed to be close to the ideal bulk structure[25].

Spectroscopic-grade benzene was introduced into a glass and stainless-steel gas manifold. The benzene sample was degassed by freezing the sample, pumping over it and then thawing the sample. This procedure was repeated several times. Benzene was introduced into the UHV chamber through a leak valve and a stainless doser tube 0.15mm in diameter. (The vapor pressure of benzene at room temperature is $\sim$ 100 torr.)

When the Pd(111) sample was exposed to several Langmuirs (L) of benzene to form a saturated monolayer at room temperature, only fuzzy ring-like LEED patterns were seen around the integral order spots, indicating that the benzene overlayer was disordered. We tried different surface coverages, and also annealed below $\sim$150C (where benzene starts to decompose), but found no ordered superlattice.

Since CO helps to form ordered overlayers on the Rh(111) and Pt(111) surfaces, we applied the same approach to the benzene/Pd(111) system. It was difficult, however, to produce ordered surface structures on Pd(111). After many trials of dosing benzene and CO, we found a reproducible ordered (3x3) structure. This structure appeared only after a large exposure of benzene and CO[26]. Occasional heating of the crystal up to 100C *during* the synthesis seemed to help

ordering. However the final (3x3) structure was disordered by heating to 100C. Otherwise, it was stable enough to remain for weeks in the UHV chamber.

The (3x3) superstructure used in this LEED study was produced by the following procedure:

I. Exposure to 0.5L of CO at room temperature: a weak $(\sqrt{3}x\sqrt{3})R30°$-CO pattern is visible. (Exposures quoted in langmuirs have not been corrected for ion-gauge sensitivity.)

II. Exposure to 3L of benzene at room temperature: the LEED exhibits a disordered ring-like pattern.

III. Alternate dosage of benzene and CO for a total exposure of 170L and 12L, respectively, including annealing at 100C for several times: 6 spots appear around integral spots.

IV. Exposure to 120L of benzene: the (3x3) pattern starts to form.

V. Exposure to 240L of benzene: a sharp (3x3) LEED pattern is observed, as illustrated in Fig. 1.

The surface species were identified to be molecular benzene and molecular CO by HREELS[26]. The TDS was monitored at mass 2 (H_2), mass 28 (CO), and mass 78 (C_6H_6). The heating rate used was ~15K/s. The benzene molecules underwent both molecular desorption and dehydrogenation evolving H_2 and left carbon on the palladium surface like pure benzene on the Pd(111) surface. The 78 amu desorption spectrum had two distinct peaks at 370K and 520K which contrasts with the broad TDS feature observed for pure benzene overlayer. The

mass 2 (=H_2) TDS was similar to that of the pure benzene overlayer. The CO TDS peak position (~480K) was the same as for a pure CO overlayer in the $(\sqrt{3}x\sqrt{3})R30^\circ$ arrangement, however the onset of the desorption starts at a lower temperature (~350K for the (3x3) structure, compared to ~380K for the pure CO overlayer). The peak area of CO TDS was utilized to estimate the stoichiometry of the benzene-CO-palladium complex as will be discussed in section 4.

2.3. I-V Curve Measurement

LEED data were recorded at both room temperature and 120K. The main features of both data sets were very similar, except for the lower contrast in the LEED patterns at room temperature, due to the relatively low Debye temperature of palladium. At room temperature, the intensity of the overlayer spots was very weak especially at incident electron energies above 100eV. At 120K thermal diffuse scattering was reduced and the contrast in the diffraction pattern was improved, resulting in a larger range of useful I-V data. The following discussion refers to the 120K data.

The I-V data were collected at normal incidence and with the incident electron beam rotated 5° from normal incidence toward the [1, 1, $\bar{2}$] direction, which can be labeled (θ, ϕ) = (5°, 0°); this direction of tilt maintains one mirror plane of symmetry. The energy range used was 20-200eV. In order to confirm reproducibility several sets of experimental I-V curves were obtained from different sampling positions on the palladium crystal for both normal and off-normal incidence.

After symmetrically equivalent beams were averaged together within each data set, two of such data sets from different sampling positions were further averaged together to obtain the final I-V data. The final normal-incidence data set had 16 independent beams over a cumulative energy range of 1000 eV. The (5°, 0°) data set had 29 independent beams over a cumulative energy range of 1980 eV.

3. Theory

The theoretical methods which we have applied in this work were very similar to those used in the structural determination of Rh(111)-(3x3)-C_6H_6 +2CO[5].

Within the Combined Space Method[27] we have used Renormalized Forward Scattering to stack layers. The substrate layer diffraction was calculated accurately with conventional methods[27]. The overlayer diffraction matrices were obtained with Matrix Inversion within individual molecules, and Kinematic Sublayer Addition to combine the molecules. Beam Set Neglect was applied to add the overlayer to the substrate.

The non-structural parameters in our LEED calculations for the substrate were selected as described in a previous LEED study of clean and carbon monoxide-covered Pd(111)[25]. For benzene, the same phase shifts as used on Rh(111)[4,5] and Pt(111)[3] were taken. Phase shifts up to $l_{max} = 5$ were used.

For the comparison between experiment and theory, a set of five R-factor formulas and their average was used, as described previously and used by us in many prior LEED analyses[2–5,25].

4. Structure Analysis

In order to reduce the number of possible structures to be analyzed in the LEED structure search, we utilized chemical information obtained with HREELS and TDS. HREELS indicated that benzene adsorbs molecularly parallel to the surface, whether with[26] or without[17,18] coadsorbed CO. This orientation restricted the number of benzene molecules per (3x3) unit cell to be only one, by taking the Van der Waals sizes of benzene molecules into account. CO was molecularly adsorbed perpendicular to surface according to the HREELS data[26]. CO TDS detected about one third of a monolayer of CO, corresponding to three CO molecules per unit cell[26]. However the Van der Waals size consideration allows a maximum of two upright CO molecules per unit cell. Therefore, the number of CO per unit cell was set to be two, the same number found in the corresponding (3x3) structure on Rh(111). The excess CO can be at defect sites of our Pd(111) sample, or in the disordered region outside of the major (3x3) phase. (We frequently observed disordered regions, by moving the LEED electron beam across the Pd(111) sample, especially near the edge of the crystal.) Thus, our analyses are based on the model with one flat-lying benzene and two upright CO molecules at high symmetry adsorption sites in the (3x3) unit cell.

Our structural search for Pd(111)-(3x3)-C_6H_6+ 2CO was very similar to that used in our analysis for Rh(111)-(3x3)-C_6H_6+2CO. We tested approximately 1500 distinct structures as shown in Table 1. In a first stage of the structural determination (Table 1 - A,B,C,D), the carbon ring was given its gas-phase geometry (hexagonal symmetry with equal C-C bond lengths of 1.397Å) and the C-O bond

lengths were fixed at 1.15Å. This allowed the adsorption sites and molecular distances from the metal to be approximately determined. Here we assumed that benzene and CO are adsorbed over the same kind of high-symmetry sites, as estimated by their Van der Waals sizes (See Figure 2b,c). The structure where both benzene and CO adsorb over fcc-hollow sites was clearly favored by R-factor comparison as shown in Table 2. Two high-symmetry azimuthal (Φ) orientations of the benzene molecules were also investigated (See Table 1-C1, C2, Fig. 2a, and Fib. 2b). The angle Φ was confirmed to be 0°, as Van der Waals sizes would indicate (Fig. 2b).

Then, in the favored fcc-hollow site and with Φ= 0°, we examined possible substrate relaxations (Table 1-E), since we had observed small relaxations for clean and CO-covered Pd(111) surfaces[25]. In the present case, the 1st and 2nd layer spacings were found to be expanded by +0.05Å with respect to the bulk value.

In trials F-J (Table 1), more precise analyses were conducted to determine the bond lengths and bond angles within the overlayer. In-plane Kekulé-type distortions of the C_6 ring of benzene observed on Rh(111) surface were also extensively investigated on Pd(111) surface. These consist of alternating long and short C-C bonds within the C_6 rings, with C_{3v} symmetry. Two variables can be used to describe such distortions (see Figure 2d): a C_6 ring radius r and an angular departure β from 6-fold symmetrical positions. Note that in the preferred benzene adsorption sites (fcc-hollow) and with $\Phi = 0$, the Kekulé distortion has the same symmetry as the metal site itself. R-factor plots as a function of r and

as a function of β are shown in Figure 3a and 3b, respectively. They illustrate that the LEED analysis is sensitive to the distortion of the benzene molecules. The R-factor minima (C_6 radius (r) =1.43 $\pm$ 0.10 Å, and $\beta = \sim 0.75$ °) yielded the following C-C bond lengths of the C_6 ring skeleton:

$$d_1 = 2r\sin(30° - \beta) = 1.40 \pm 0.10 \text{ Å}$$

$$d_2 = 2r\sin(30° + \beta) = 1.46 \pm 0.10 \text{ Å}$$

(d_1 and d_2 are defined in Figure 2; the C-C bond with the shorter bond length d_1 is positioned over one palladium atom, whereas the C-C bonds with the longer bond length d_2 is positioned bridging two palladium atoms.)

The other three structural variables, the perpendicular metal-carbon separations for CO and benzene and the CO bond length, were determined by similar R-factor analyses in the course of trials F-J. A few theoretical I-V curves corresponding to the grid point nearest the minimum R-factor are shown in Fig. 4, along with experimental I-V curves.

5. Results

Our best structure for Pd(111)-(3x3)-C_6H_6 + 2CO, i.e., the structure which minimizes the R-factors, is illustrated in Fig. 5. The hydrogen atom positions are guessed, since they were not determined by LEED. (Some theoretical calculations indicate[28,29] that, when benzene is adsorbed on transition metals, hydrogen atoms point away from the substrate surface, perhaps due to rehybridization of the carbon atoms and/or electrostatic repulsive interactions between the hydrogen atoms

and metal surfaces.) In the (3x3) structure, both benzene and CO are centered over 3-fold fcc-type hollow sites in a compact arrangement. The benzene carbon ring has a spacing of 2.25 ± 0.05 Å to the metal surface with six identical Pd-C bond lengths of 2.39 ± 0.05 Å. No significant in-plane distortion has been detected within the error bars: we find C-C distances of $d_1 = 1.40 \pm 0.10$ Å, and $d_2 = 1.46 \pm 0.10$ Å (d_1 and d_2 are defined in Fig. 2). However, the possible deviations from the gas-phase benzene structure (d_1=d_2=1.397Å) are in the same direction as those on Rh(111): shorter C-C bonds over individual metal atoms and longer C-C bonds bridging two metal atoms. The CO molecular axis is perpendicular to the surface, the C-O and Pd-C bond lengths being 1.17 ± 0.05 Å and 2.05 ± 0.04 Å, respectively.

The optimal muffin-tin zero level, assumed layer-independent, is found to be 9±1eV below vacuum. The minimized value of the five-R-factor average is 0.25, while the corresponding Zanazzi-Jona and Pendry R-factor values are 0.49 and 0.48 (using the normal-incidence data only). These R-factor values are comparable to values obtained for similar coadsorption structures: Rh(111)-c($2\sqrt{3}$x4)*rect*-C_6H_6+CO with R(average)=0.31, R(Zanazzi-Jona)=0.40, R(Pendry)=0.66, Rh(111)-(3x3)-C_6H_6 +2CO with R(average)=0.21, R(Zanazzi-Jona)=0.24, R(Pendry)=0.41, and Pt(111)-($2\sqrt{3}$x4)*rect*-$2C_6H_6$ + 2CO with R(average)=0.28, R(Zanazzi-Jona)=0.42, R(Pendry)=0.54. The results are summarized in the format of SCIS (Surface Crystallographic Information Service[1]) in Table 3.

6. Discussion

The first structure analysis of coadsorbed benzene and CO on Pd(111) has been performed by LEED with a minimum R-factor of 0.25. This result gives an unique opportunity to compare similar coadsorption structures of benzene+CO on three different metal surfaces: Pd(111), Rh(111), and Pt(111). Table 4 gathers pertinent data for these structures, while Fig. 6 shows their analogies and differences.

6.1. Coadsorption-Induced Ordering

The present benzene/CO structure illustrates that coadsorption can produce new surface periodicities which cannot be formed by the pure component adsorbates taken separately. At room temperature, pure CO presents two ordered structures[30]: $(\sqrt{3}x\sqrt{3})R30^\circ$ at $\theta = 1/3$ and c(4x2) at $\theta = 1/2$. On the other hand, pure benzene is disordered at any surface coverage. Coadsorption of these two molecules resulted in the (3x3) structure.

Coadsorption-induced ordering of organic overlayers has already been reported on Rh(111) and Pt(111) surfaces for a variety of pairs of adsorbates[3–6,31,32]. On the Pt(111) surface, benzene by itself does not order[3,6,21,32], just as on Pd(111), but four ordered structures have been observed by coadsorbing CO[3,6,32]. On Rh(111), benzene by itself orders weakly[6,20] (electron-beam-induced disordering is rapid), while several stable ordered coadsorbed structures are observed by LEED in the presence of CO[4,5,6]. There has been no theoretical work concerning energetics of such coadsorption induced ordering, however one

model for explaining this ordering behavior is that benzene and CO act like donors and acceptors, respectively, with respect to the substrate metal, and that donors are surrounded by acceptors and vice versa, in a way similar to an ionic crystal. The donor/acceptor character is suggested by work function measurements for coadsorption on Pt(111)[32,33] and Rh(111)[34].

6.1.1. Charge transfer from Pd(111) to CO

It is known that, on the Pt(111) surface, CO switches its adsorption site from 1-fold to 2-fold and possibly to 3-fold as the amount of coadsorbed potassium is increased[35]. This indicates that the preferred CO adsorption site is closely related to the work function of the substrate(potassium decreases the work function by charge transfer to the metal). On the Pd(111) surface, pure CO at coverages up to 1/3 monolayers prefers to adsorb at the 3-fold site[25], since the work function of clean Pd(111) is less than that of Pt(111)[36]. However, upon increasing the CO coverage, CO switches its adsorption site from 3-fold to 2-fold, and at low temperatures the 1-fold site is attainable[31,37]. The same effect has been observed on palladium crystallites supported on SiO_2, and it is interpreted in terms of charge transfer from palladium to adsorbed CO[38]. Thus CO itself seems to work as a net electron-acceptor on Pd(111). Consistent with this conclusion, the adsorption of CO increases the work function of the Pd(111) crystal surface[39,40].

6.1.2. Coadsorption effects of benzene and CO on Pd(111)

It is believed that benzene is a net electron-donor to the Rh(111) and Pt(111) surfaces, based on work-function measurements[32,33,34], on the reduction of the CO stretching frequency[6] when coadsorbed with benzene, and also on the fact that CO switches its adsorption site from 1-fold to 2-fold or 3-fold on these surfaces when benzene is coadsorbed[3,4,5]. Furthermore, a theoretical study on the Rh(111) surface[28] has suggested that benzene is a net electron donor to Rh(111).

Whether benzene is a net donor or acceptor toward Pd(111) is not clear. However, the large decrease in the CO stretching frequency when coadsorbed with benzene[26] might be caused by the enhanced backdonation from the palladium to the $2\pi^*$ orbital of adsorbed CO because of the coadsorbed benzene. Also, the 3-fold site of CO on Pd(111) when coadsorbed with benzene is consistent in this context.

So far the CO-induced ordering of benzene has been found on three different metal surfaces, including Pd(111), and the charge transfer between substrate and coadsorbates seems to play an important role in causing this phenomenon.

6.2. The Structure of Carbon Monoxide

The (3x3) unit cell contains two CO molecules, corresponding to a surface coverage of 2/9, located on 3-fold fcc-hollow sites. Pure CO is known from LEED[25] to also be adsorbed on 3-fold fcc-hollow sites at $\theta = 1/3$ (at higher coverages, a shift to bridge sites occurs[30,37]). This is consistent with the tendency known on Pt(111) and Rh(111) for CO to move to higher-coordination sites (at

least when available) in the presence of donors such as benzene or alkali atoms[3,4,5,35]. Note that CO on Rh(111) is adsorbed at another kind of hollow site (hcp-hollow) in the benzene coadsorption structures.

The CO bond is perhaps slightly elongated due to coadsorbed benzene: 1.17±0.05Å in the (3x3) structure vs. 1.15±0.05Å in the pure CO overlayer[25] and 1.15Å in the gas phase. At the same time a significant reduction of the CO stretching frequency has been observed by HREELS: from about 1840 cm^{-1} to about 1750 cm^{-1}. The right part of the Fig. 7 shows C-O bond lengths on various metal substrates, as primarily obtained by LEED. We see that the C-O bond lengths increase as the coordination number increases; the amount of change is, however, rather small. The left part of this figure also shows metal-carbon bond lengths for CO on various metal substrates. This quantity varies appreciably, as the coordination number increases. The results on Pd(111) fit the general trend well.

6.3. The Structure of Benzene

6.3.1. Position of Benzene Relative to Pd(111)

Benzene is found to be adsorbed molecularly over a fcc-hollow site in the (3x3) structure. Pure disordered benzene is thought to adsorb over a bridge site of Pd(111), based on the similarity of HREELS for benzene on Pd(111) and Pd(100)[17]. Our result implies, therefore, that the benzene molecules switch their adsorption site from bridge to fcc-hollow when coadsorbed with CO. A similar

switching occurs on Rh(111), but the hcp-hollow site rather than the fcc-hollow site is found on that surface. The metal-carbon bond lengths for benzene on Pd(111) are found to be 2.39±0.05Å. This value is to be compared with 2.30±0.05Å and 2.35±0.05Å on Rh(111) and 2.25±0.05Å on Pt(111) (See Table 4). Thus there is a clear trend towards stronger metal-carbon bonding from Pd to Rh to Pt.

6.3.2. Benzene Ring Distortions

On Pd(111) (with coadsorbed CO), the benzene ring skeleton is found to be essentially indistinguishable from the gas phase structure within the error bar (±0.10Å). There may be a slight C_6 ring expansion to a radius of 1.43±0.10Å and a Kekulé distortion with a difference between C-C bonds of 0.06±0.10Å. This contrasts with benzene on Rh(111) or Pt(111) which showed significant in-plane distortions(See Table 4).

The benzene-transition metal interactions can be understood in the framework of d-π interaction analogous to coordination chemistry[28,41]. This interaction results in a benzene ring expansion, which increases with the metal-carbon bond strength. Table 4 shows such a trend from Pd(111) via Rh(111) to Pt(111). This trend parallels the decrease in benzene-metal bond length mentioned above.

On Rh(111) and Pt(111), where a strong benzene-metal interaction has been detected by LEED, the benzene rings exhibit long and short C-C bonds within the molecule. In these cases the benzene molecules adopt the same symmetry as their adsorption sites: thus, benzene adsorbed at bridge sites on Pt(111) show an in-

plane distortion with C_{2v} symmetry, and benzene adsorbed at hollow sites on Rh(111) shows a Kekulé distortion with C_{3v} symmetry. It is therefore very probable that at least a weak Kekulé-type distortion exists in the case of Pd(111), although it is too small to be confirmed by LEED.

These trends are further supported by HREELS data[6,26] where the γ_{CH} mode frequency increases monotonously from the gas phase value (~670 cm^{-1}) upon adsorption of benzene on Pd(111), Rh(111), and Pt(111): the respective frequencies are 730-770cm^{-1} on Pd(111), 780-810cm^{-1} on Rh(111) and 830-850cm^{-1} on Pt(111). These frequencies include both pure benzene overlayers and coadsorbed overlayers of benzene and CO. The coadsorbed CO affects the γ_{CH} mode frequency of adsorbed benzene. However, such indirect interactions between adsorbates are less effective in changing the γ_{CH} frequency than switching substrates from Pd to Rh to Pt. Thus the trends of benzene-metal interaction obtained from benzene-CO-metal systems will presumably hold qualitatively in the case of pure benzene on Pd(111), Rh(111), and Pt(111) surfaces.

6.3.3. Chemical Properties

In this section, we explore the correlation between the structural bond-lengths information obtained by LEED with bond energies and catalytic properties. TDS data were gathered from various references, but because of different experimental conditions, only qualitative comparisons can be made for TDS data of different metals.

When the adsorbed benzene is heated, decomposition and molecular desorption are the competing processes on Pd(111), Rh(111), and Pt(111) surfaces. Koel et al.[42] have proposed, based on TDS and HREELS data, that benzene decomposes on Rh(111) via an acetylene-like intermediate (which however is very short-lived at the benzene decomposition temperature). Interestingly, on supported Rh particles, acetylene can be formed from benzene with coadsorbed CO[43]. This might be related to the strong benzene-metal interaction and the resulting Kekulé distortion detected by LEED.

Benzene chemisorbed on the Pt(111) crystal is less asymmetrically distorted, exhibiting a more uniform expansion of the ring. This structure may suggest a benzene intermediate on the metal surface that can desorb intact at the higher temperatures and pressures of the catalytic reaction[3].

The benzene on Pd(111) surface was found by LEED to be weakly distorted. On this surface, a higher activation energy for decomposition is apparent: the H_2 desorption maximum due to benzene decomposition is higher on Pd(111)(~555K) than Rh(111)(~490K[42]) or Pt(111)(~545K[44,45]). This seems to correlate with the weaker benzene-palladium interaction observed by LEED. Molecular benzene desorbs from Pd(111) at the two temperature of ~430K and ~530K[17]. This indicates that benzene still exist as an intact molecule on the surface at 530K. (By contrast, Rh(111) has only a 395K desorption peak[42] and Pt(111) has 375K and 450K peaks[44,45], indicating that decomposition is predominant at higher temperatures on these surfaces.)

It is known that acetylene can trimerize to form benzene on Pd(111) crystal surfaces[7–14], but not on Rh(111)[46] or on Pt(111)[47]. T.G. Rucker et. al. have studied[13] this reaction at high pressures(200 to 1200 Torr) in the temperature range of 273-573K, and found that benzene was the only product detected. This might be related to the weak benzene-palladium interaction and the resulting easy molecular benzene desorption at these reaction conditions.

The cyclotrimerization occurs on Pd(111) even under UHV conditions, and benzene desorbs at 250K and 490K after adsorbing acetylene at 130K and subsequent heating. The Pd(111)-(3x3)-C_6H_6+2CO structure was obtained above room temperature. Structural studies on both acetylene and benzene at low temperatures are necessary to understand such low-temperature benzene formation.

7. Conclusion

An ordered (3x3) benzene overlayer was formed on Pd(111) by coadsorbing benzene and CO. A dynamical LEED analysis has revealed that both benzene and CO bond over fcc-type hollow sites in a close-packed form with a 2:1 CO to C_6H_6 stoichiometry.

Weak distortions from the gas phase geometry may be present in both molecules. This contrasts with larger benzene distortion on Rh(111) and Pt(111). Clear trends emerge which indicate an increasing metal-benzene bond strength and decreasing C-C bond strength in going from Pd(111) via Rh(111) to Pt(111). These trends are consistent with vibrational spectroscopy results.

Acknowledgements

We thank C.M. Mate, D. F. Ogletree, C. Minot, and E.L. Garfunkel for fruitful discussions and assistance. This work was supported by the Director, Office of Energy Research, Office of Basic Energy Sciences, Materials Sciences Division, of the U.S. Department of Energy under contract No. DE-AC03-76SF00098. We also acknowledge supercomputer time provided by the Office of Energy Research of the U.S. Department of Energy and NATO for an US-France exchange grant. H. Ohtani gratefully acknowledges financial support from IBM Japan.

References

1 MacLaren, J. M.; Pendry, J. B.; Rous, R. J.; Saldin, D. K.; Somorjai, G. A.; Van Hove, M. A.; Vvedensky, D. D. "Surface Crystallographic Information Service: A Handbook of Surface Structures" Reidel: Dordrecht, 1987.

2 Van Hove, M. A.; Lin, R. F.; Somorjai, G. A. *Phys. Rev. Lett.* **1983,** *51,* 778.

3 Ogletree, D. F.; Van Hove, M. A.; Somorjai, G. A. *Surf. Sci.* **1987**, *183*, 1.

4 Van Hove, M. A.; Lin, R. F.; Somorjai, G. A. *J. Am. Chem. Sci.* **1986**, *108*, 2532.

5 Lin, R. F.; Blackmann, G. S.; Van Hove, M. A.; Somorjai, G. A. *Acta Crystallographica,* **1987**, *B43*, 368.

6 Mate, C. M.; Somorjai, G. A. *Surf. Sci.* **1985**, *160*, 542.

7 Sesselmann, W.; Woratschek, B.; Ertl, G.; Küppers, J.; Haberland, H. *Surface Sci.* **1983**, *130*, 245.

8 Tysoe, W. T.; Nyberg, G. L.; Lambert, R. M. *J. Chem. Soc. Chem. Commun.* **1983**, 623.

9 Tysoe, W. T.; Nyberg, G. L.; Lambert, R. M. *Surface Sci.* **1983**, *135*, 128.

10 Gentle, T. M.; Muetterties, E. L. *J. Phys. Chem.* **1983**, *87*, 2469.

11 Gentle, T. M.; Grassian, V. H.; Klarup, D. G.; Muetterties, E. L. *J. Am. Chem. Soc.* **1983**, *105*, 6766.

12 Marchon, B. *Surface Sci.* **1985**, *162*, 382.

13 Rucker, T. G.; Logan, M. A.; Gentle, T. M.; Muetterties, E. L.; Somorjai, G. A. *J. Phys. Chem.* **1986**, *90*, 2703.

14 Logan, M. A.; Rucker, T. G.; Gentle, T. M.; Muetterties, E. L.; Somorjai, G. A. *J. Phys. Chem.* **1986**, *90*, 2709.

15 Lloyd, D. R.; Quinn, C. M.; Richardson, N. V. *Solid State Comm.* **1977**, *23*, 141.

16 Netzer, F. P.; Mack, J. U. *J. Chem. Phys.* **1983**, *79*, 1017.

17 Waddill, G. D.; Kesmodel, L. L. *Phys. Rev. B,* **1985**, *31*, 4940.

18 Waddill, G. D.; Kesmodel, L. L. *Phys. Rev. B,* **1985**, *32*, 2107.

19 Grassian, V. H.; Muetterties, E. L. *J. Phys. Chem.* **1987**, *91*, 389.

20 Koel, B. E.; Crowell, J. E.; Mate, C. M.; Somorjai, G. A. *J. Phys. Chem.* **1984**, *88*, 1988.

21 Lehwald, S.; Ibach, H.; Demuth, J. E. *Surface Sci.* **1978**, *78*, 577.

22 Ogletree, D. F.; Somorjai, G. A.; Katz, J. E., *Rev. Sci. Instruments,* **1986**, *57*, 3012.

23 Kesmodel, L. K.; Somorjai, G. A. *Phys. Rev.* **1975**, *B11*, 630.

24 Gentle, T. M. Ph.D. Thesis, University of California–Berkeley, 1984.

25 Ohtani, H.; Van Hove, M. A.; Somorjai, G. A. *Surface Sci,* **1987**, *187*, 372.

26 Ohtani, H.; Bent, B. E.; Mate, C. M.; Van Hove, M. A.; Somorjai, G. A. *Appl. Surf. Sci.* in press, and to be published.

27 Van Hove, M. A.; Tong, S. Y. "Surface Crystallography by LEED", Springer: Heidelberg, 1979.

28 Garfunkel, E. L.; Minot, C.; Gavezzotti, A.; Simonetta, M. *Surface Sci.* **1986**, *167*, 177.

29 Bagus, P. private communication.

30 Bradshaw, A. M.; Hoffmann, F. M.; *Surface Sci.* **1978**, *72*, 513.

31 Mate, C. M.; Bent, B. E.; Somorjai, G. A. *J. Electron Spectroscopy and Related Phenomena,* **1986**, *39*, 205.

32 Ogletree, D. F. Ph.D. Thesis, University of California—Berkeley, 1986.

33 Gland, J. L.; Somorjai, G. A.; *Surface Sci.* **1973**, *38*, 157.

34 Mate, C. M. Ph.D. Thesis, University of California—Berkeley, 1986, and to be published.

35 Garfunkel, E. L.; Crowell, J. E.; Somorjai, G. A. *J. Phys. Chem.* **1982**, *86*, 310.

36 Anderson, A. B.; Awad, M. K. *J. Am. Chem. Soc.* **1985**, *107*, 7854.

37 Hoffmann, F. M.; Ortega, A. *Proc. 1st Intern. Conf. on Vibrations in Adsorbed Layers*, Jülich 1978, KFA Jülich Report JUL-CONF-26, **1978**, 128.

38 Gelin, P.; Siedle, A. R.; Yates, J. T. *J. Phys. Chem.* **1984**, *88*, 2978.

39 Ertl, G.; Koch, J. *Z. Naturforsch.* **1970**, *25a*, 1906.

40 Ertl, G.; Koch, J. "*Adsorption-Desorption Phenomena*", ed. F. Ricca, Academic Press: New York, 345.

41 Idrissi-Rachidi, I. E.; Minot, C.; Van Hove, M. A.; Somorjai, G. A. to be published.

42 Koel, B. E.; Crowell, J. E.; Bent, B. E.; Mate, C. M.; Somorjai, G. A. *J. Phys. Chem.* **1986**, *90*, 2709.

43 Parker, W. L.; Hexter, R. M.; Siedle, A. R. *J. Am. Chem. Soc.* **1985**, *107*, 4584.

44 Tsai, M. -C.; Muetterties, E. L. *J. Am. Chem. Soc.* **1982**, *104*, 2534.

45 Garfunkel, E. L.; Maj, J. J.; Frost, J. C.; Farias, M. H.; Somorjai, G. A. *J. Phys. Chem.* **1983**, *87*, 3629.

46 Mate, C. M. private communication.

47 Kang, D. B.; Anderson, A. B. *Surface Sci.* **1985**, *155*, 639, and references therein.

48 Gomez-Sal, M. P; Johnson, B. F. G.; Lewis, T.; Raithby, P. R.; Wright, A. H. *J. Chem. Soc. Chem. Commun,* **1985**, 1682.

TABLE 1. Test structures for Pd(111)-(3x3)-C_6H_6+2CO

	Benzene					CO			Pd(111)	Incidence Directions
				C_6 ring distortions[d]						
	site[a]	Φ(°)[b]	$d_{\perp C_{ave}-C_6}$(Å)[c]	r(Å)	β(°)	site	$d_{\perp Pd-C}$(Å)[e]	d_{C-O}(Å)[f]	$\Delta d_{\perp Pd-Pd}$(Å)[g]	(θ,ϕ)(°)[h]
A	top	0	–0.6(.2)0.0	1.397	0	top	1.4(.05)1.65	1.15	0	(0,0)
B	bridge	0,30	0.5(.2)1.1	1.397	0	bridge	1.5(.1)2.0	1.15	0	(0,0),(5,0),(5,180)
C1	fcc-hollow	0	0.7(.2)1.3	1.397	0	fcc-hollow	1.2(.05)1.45	1.15	0	(0,0),(4,0),(5,0),(6,0),(5,180)
C2	fcc-hollow	30	0.7(.2)1.3	1.397	0	fcc-hollow	1.2(.05)1.45	1.15	0	(0,0)
D	hcp-hollow	0	0.7(.2)1.3	1.397	0	hcp-hollow	1.2(.05)1.45	1.15	0	(0,0)
E	fcc-hollow	0	0.7(.2)1.3	1.397	0	fcc-hollow	1.2(.05)1.45	1.15	.05(.05).15	(0,0),(5,0)
F	fcc-hollow	0	0.9(.05)1.0	1.2(.17)1.71	–4(4)4	fcc-hollow	1.25(.05)1.45	1.15	.05	(0,0),(5,0)
G	fcc-hollow	0	0.9(.05)1.0	1.2(.17)1.71	–4(4)4	fcc-hollow	1.25(.05)1.45	1.1	.05	(5,0)
H	fcc-hollow	0	1.0	1.2(.17)1.71	0	fcc-hollow	1.25(.05)1.45	1.1,1.2,1.25	.05	(0,0)
I	fcc-hollow	0	0.7(.2)1.3	1.2(.17)1.71	–4(4)4	fcc-hollow	1.2(.05)1.45	1.15	.05	(0,0)
J	fcc-hollow	0	0.7(.2)1.3	1.435	–4(4)4	fcc-hollow	1.2(.05)1.45	1.15	.05	(0,0)

Notes

a The site over which the carbon ring is centered.

b The azimuthal orientation of the benzene ring, as defined in Figure 2.

c Smallest layer spacing between C of CO and C_6 carbons of C_6H_6. The first and last numbers give the range of layer spacings in Å, and the number in parentheses is the incremental step size. For example the first entry -0.6(.2)0.0

means that LEED calculations were made for carbon(CO)-carbon(C_6H_6) layer spacings of -0.6, -0.4, -0.2, and 0.0Å.

d In-plane Kekulé distortions characterized by r and β, as defined in Fig. 2.

e Perpendicular distance between topmost Pd layer and C of CO. The first and last numbers give the range of layer spacings in Å, and the number in parentheses is the incremental step size.

f C-O bond length (C-O bond always perpendicular to surface).

g Perpendiular distance between 1st and 2nd Pd layers. Positive values indicate expansions.

h Incidence directions used in theory. θ=4° and 6° correspond to checks on the accuracy of the experimental polar angle. ϕ=180° corresponds to checks on the orientation of the substrate.

TABLE 2. R-factor comparison for CO and benzene adsorbed at different sites, keeping the substrate bulk-like.

Adsorption Sites for C_6H_6 and CO (See Fig. 2 - c)		Minimum 5-Average R-Factor
A	aABC (top)	0.4338
B	dABC (bridge)	0.3008
C	cABC (fcc-hollow)	0.2696
D	bABC (hcp-hollow)	0.4060

TABLE 3. Structure Result in Format of Surface Crystallographic Information Service (SCIS)[1]

SURFACE: Substrate Face: Pd(111); Adsorbate: C_6H_6, CO
Surface Pattern: (3x3), (3,0/0,3)
STRUCTURE: Bulk Structure: fcc; Temp: 150K; Adsorbate State: Molecular;
Coverage: 1/9 (C_6H_6/Pd), 2/9 (CO/Pd)
REFERENCE UNIT CELL: a=8.25Å; b=8.25Å; A(a,b)=60°

Layer	Atom	Atom Positions		Normal Layer Spacing
A1	O	0.2222	0.2222	0.00
A2	O	0.8889	0.8889	0.22
A3	C	0.5582	0.7276	0.00
A4	C	0.7276	0.5582	0.00
A5	C	0.7276	0.3809	0.00
A6	C	0.5582	0.3809	0.00
A7	C	0.3809	0.5582	0.00
A8	C	0.3809	0.7276	0.95
A9	C	0.2222	0.2222	0.00
A10	C	0.8889	0.8889	1.30
S1	Pd	0.0000	0.0000	0.00
S2	Pd	0.3333	0.0000	0.00
S3	Pd	0.6667	0.0000	0.00
S4	Pd	0.0000	0.3333	0.00
S5	Pd	0.3333	0.3333	0.00
S6	Pd	0.6667	0.3333	0.00
S7	Pd	0.0000	0.6667	0.00
S8	Pd	0.3333	0.6667	0.00
S9	Pd	0.6667	0.6667	2.30
S10	Pd	0.1111	0.1111	0.00
S11	Pd	0.4444	0.1111	0.00
S12	Pd	0.7778	0.1111	0.00
S13	Pd	0.1111	0.4444	0.00
S14	Pd	0.4444	0.4444	0.00
S15	Pd	0.7778	0.4444	0.00
S16	Pd	0.1111	0.7778	0.00
S17	Pd	0.4444	0.7778	0.00
S18	Pd	0.7778	0.7778	2.30

2D Symmetry: p3m1
Thermal Vibrations: Debye Temp=225K with double amplitude for surface atoms;
R-factor: R_{VHT}=0.25 R_{ZJ}=0.49 R_P=0.48

TABLE 4. Adsorption geometries of benzene, indicating average carbon-ring radius, C-C bond lengths (two values where long and short bond coexist), metal-carbon distances and adsorption sites of C_6H_6 ring centers

System	C_6 radius	d_{C-C} (Å)	d_{M-C} (Å)	site
benzene/surface				
Pd(111)-(3x3)-C_6H_6+2CO	1.43±0.10	1.46±0.10 1.40±0.10	2.39±0.05	fcc hollow
Rh(111)-(3x3)-C_6H_6+2CO[5]	1.51±0.15	1.58±0.15 1.46±0.15	2.30±0.05	hcp hollow
Rh(111)-c(2$\sqrt{3}$x4)*rect*-C_6H_6+CO[4]	1.65±0.15	1.81±0.15 1.33±0.15	2.35±0.05	hcp hollow
Pt(111)-(2$\sqrt{3}$x4)*rect*-2C_6H_6+4CO[3]	1.72±0.15	1.76±0.15 1.65±0.15	2.25±0.05	bridge
benzene/complex				
C_6H_6 on Ru_6, Os_3 clusters[48]	1.44	1.48 1.39	2.27-2.32	hollow
gas				
C_6H_6 molecule	1.397	1.397		
C_2H_6 molecule		1.54		
C_2H_4 molecule		1.33		
C_2H_2 molecule		1.20		

Figure captions

1) (a) A photograph of LEED pattern of Pd(111)-(3x3)-C_6H_6+2CO. The incident electron energy is 51eV. Near-normal incidence is used.
(b) Schematic representation of the LEED pattern in (a).
(c) A (3x3) surface unit cell for a (3x3) overlayer on Pd(111) in real space.

2) Panels (a) and (b) show the molecular packing within the (3x3) overlayer on Pd(111) with the help of Van der Waals contours, for two benzene orientations ($\Phi = 0^\circ$ and 30°) and two CO molecules per unit cell. Panel (c) represents four "registries" of the (3x3) overlayer (with $\Phi = 0^\circ$) with respect to the substrate. The benzenes are represented by rings of carbons and hydrogens, the CO by crosses. Second layer palladium atoms are represented by dots in order to distinguish two kinds of hollow sites. The Kekulé distortion of benzene is defined in panel (d).

3) Five-R-factor average as a function of two of the structural parameters (r,β) describing benzene ring distortions.

4) Selected calculated LEED I-V curves at normal incidence for Pd(111)-(3x3)-C_6H_6 + 2CO for a structure near the minimum R-factor, together with experimental I-V curves.

5) The optimum structure for Pd(111)-(3x3)-C_6H_6+2CO, in side view at top and top view at bottom. Van der Waals shapes are used for overlayer molecules. The CO molecules are shown shaded. The hydrogen positions are guessed. The small dots represent the second-layer metal atoms.

6) Adsorption geometries of benzene+CO systems on Rh(111) and Pt(111) determined by LEED (Ref. [3],[4],[5])

7) The correlation between the geometries of chemisorbed CO determined by LEED and CO stretching frequency observed by IR or HREELS.

Pd (111) – (3×3) – C_6H_6 + 2 CO

LEED Pattern 51 eV

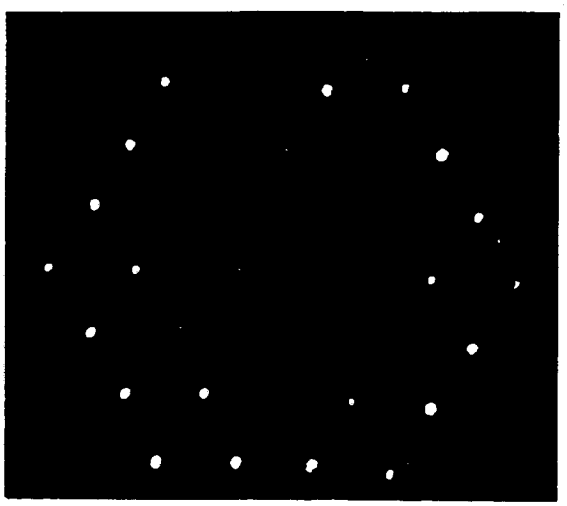

(a)

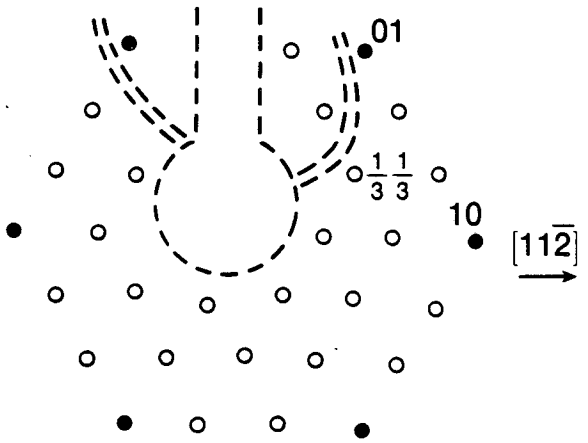

● Integral order spots
○ Fractional order spots

(b)

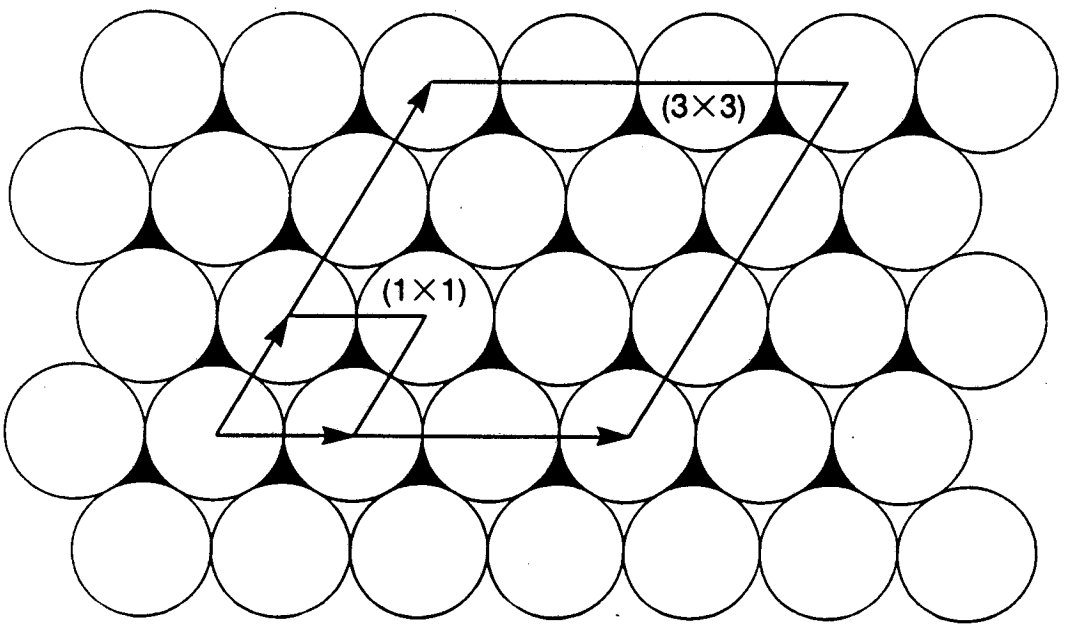

(c)

XBL 878-9078

Fig. 1

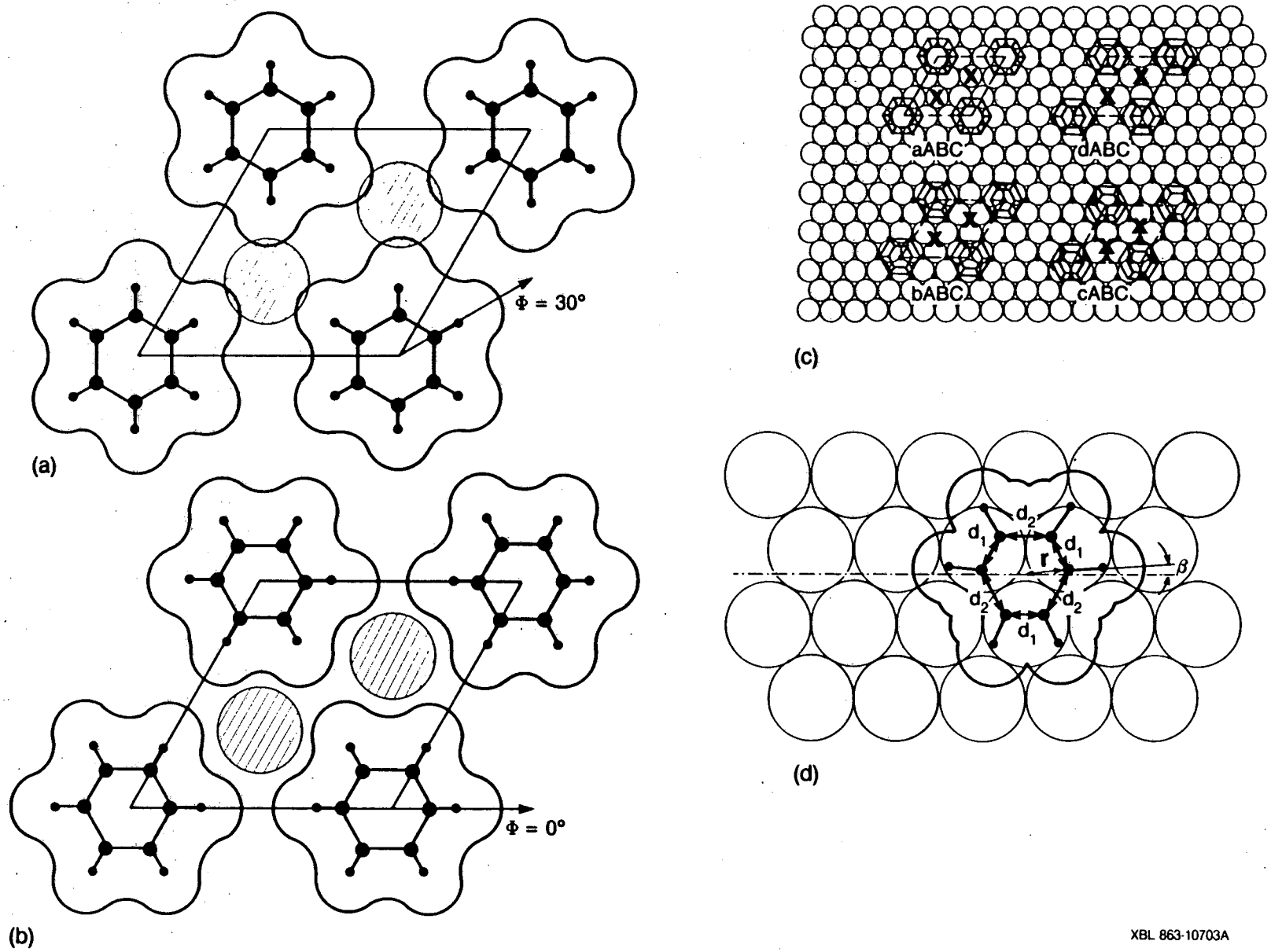

Fig. 2

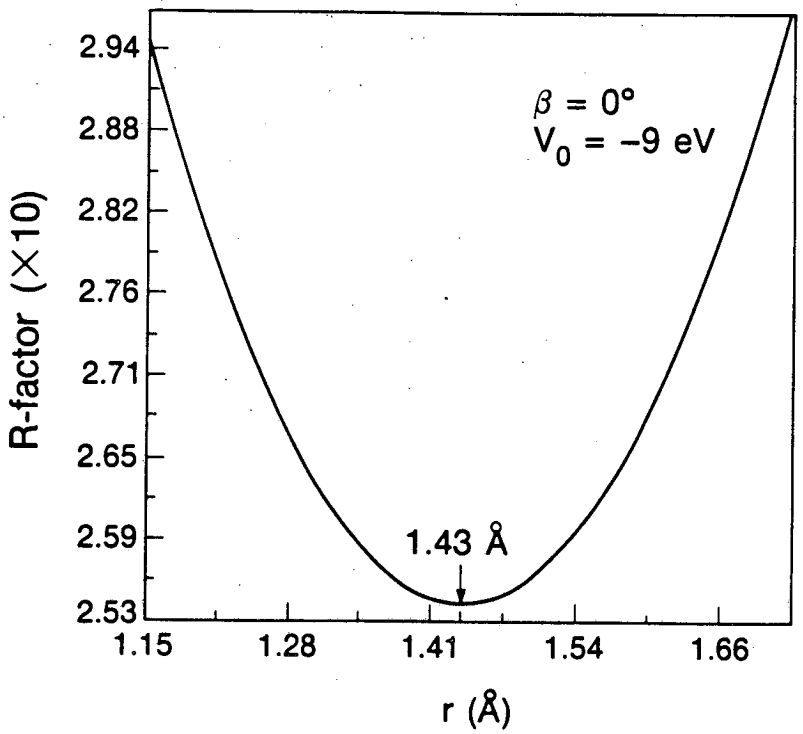

Fig.3a

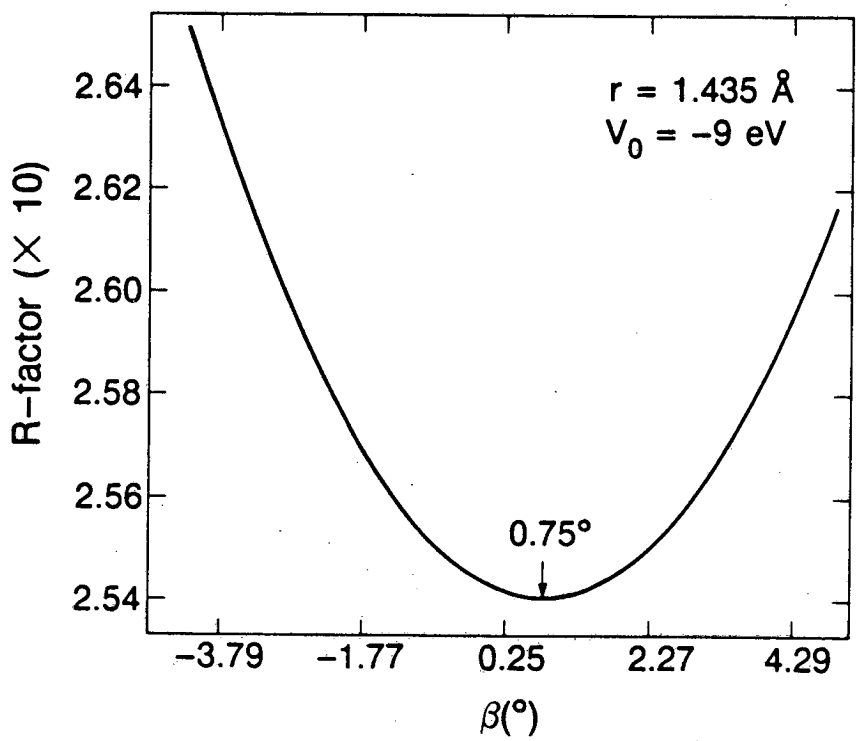

Fig.3b

XBL 879-11170

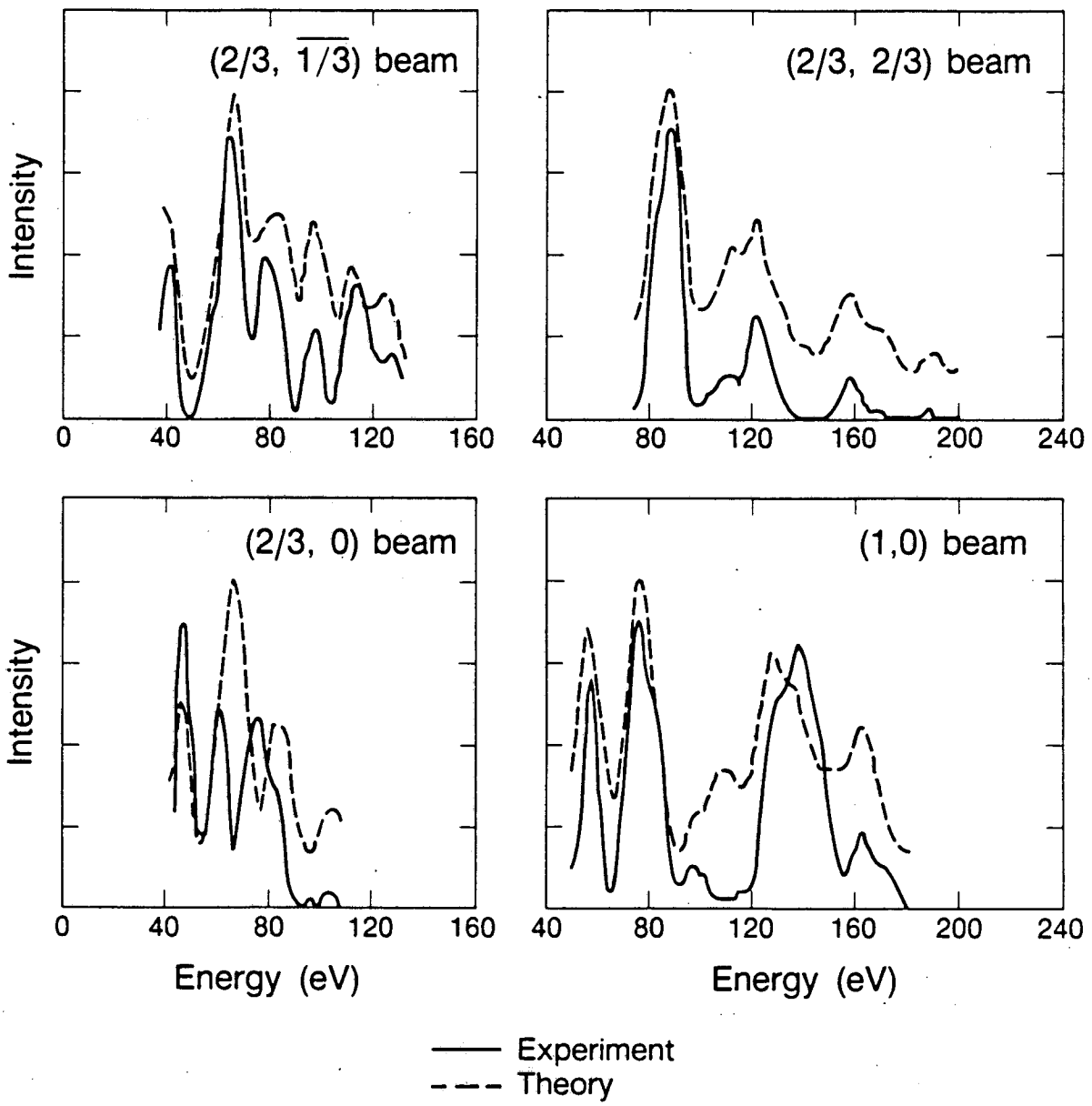

XBL 878-9074

Fig. 4

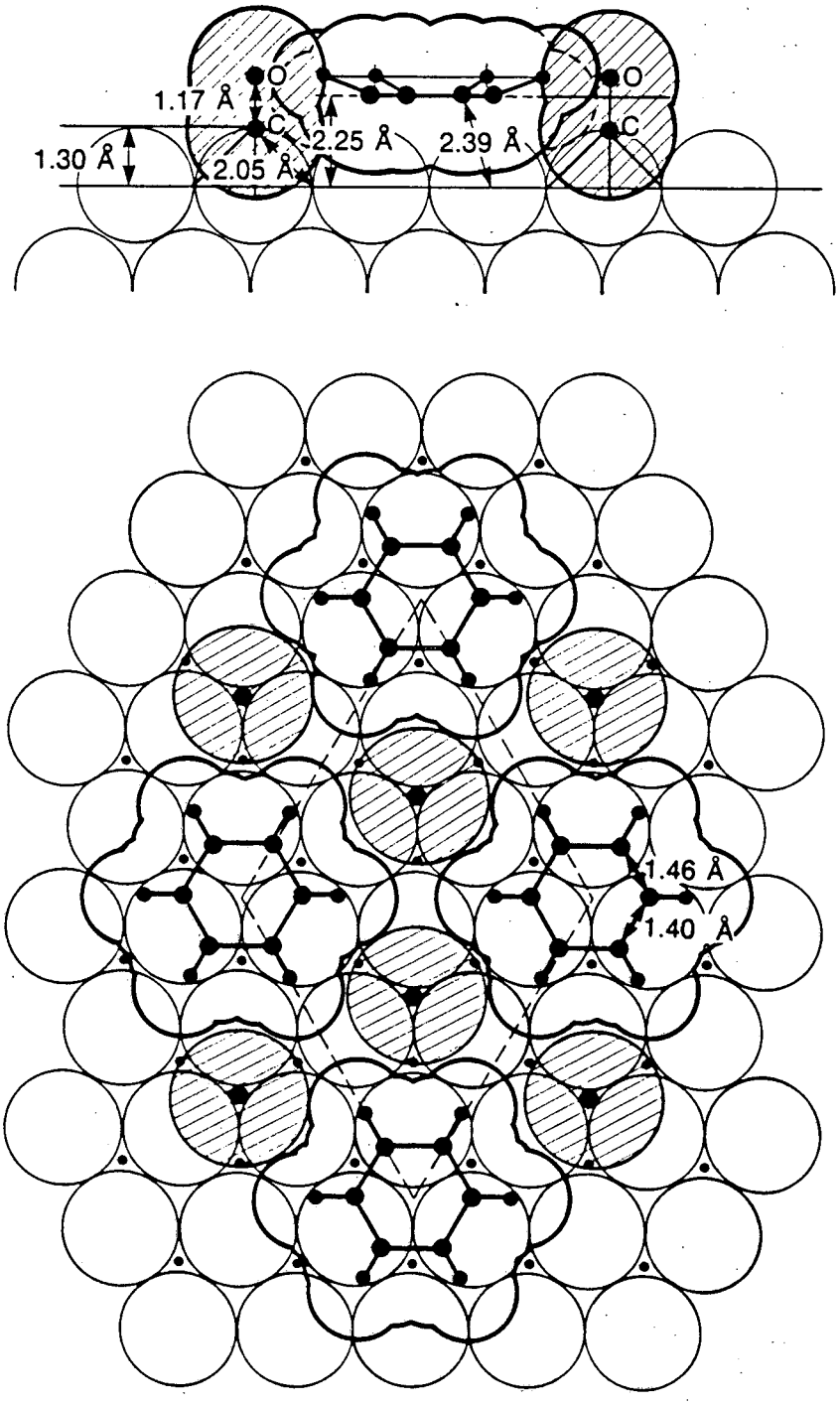

Pd (111) – (3 × 3) – C_6H_6 + 2CO

XBL 872-9565

Fig. 5

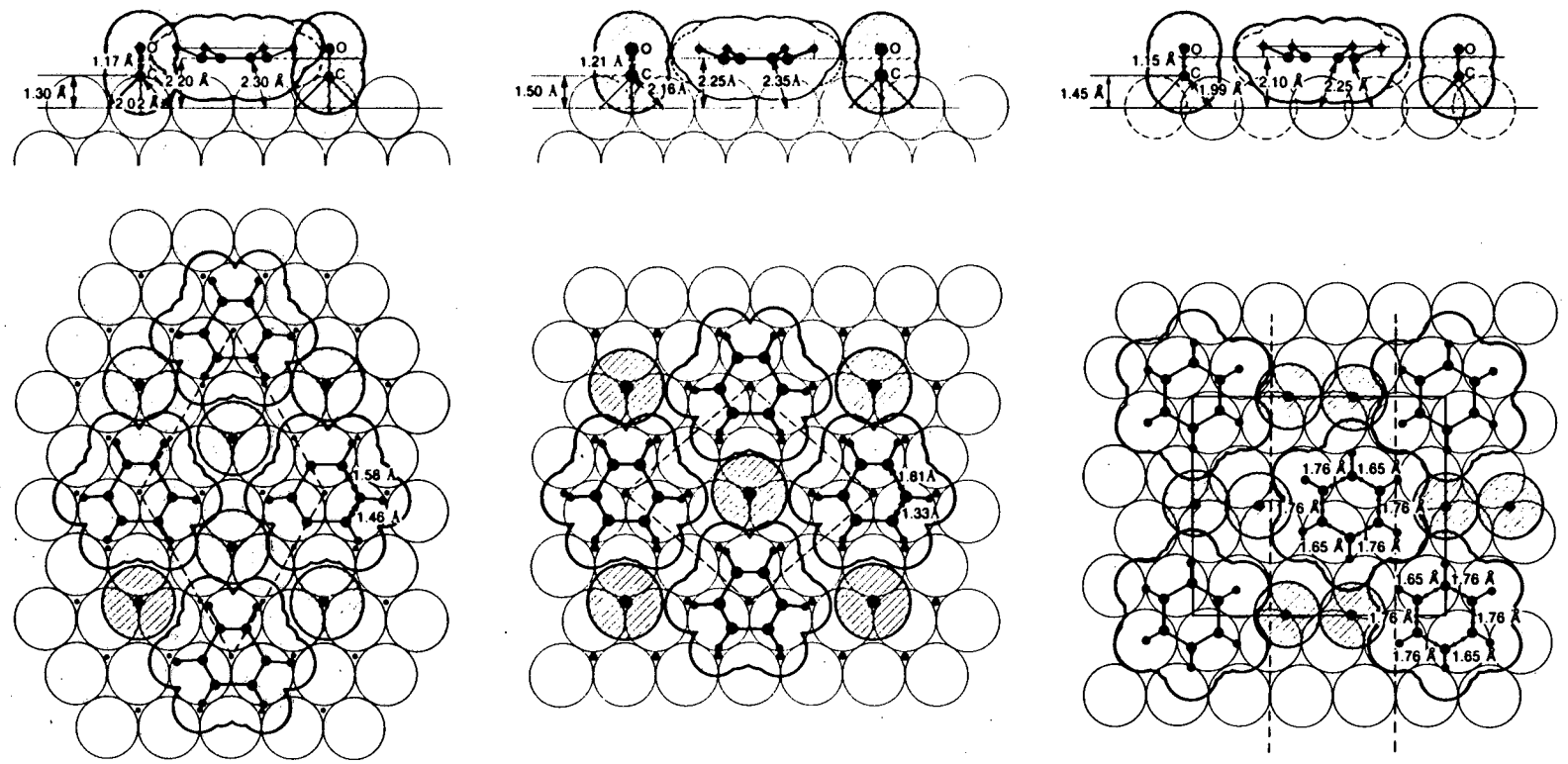

XBL 878-9075

Fig. 6

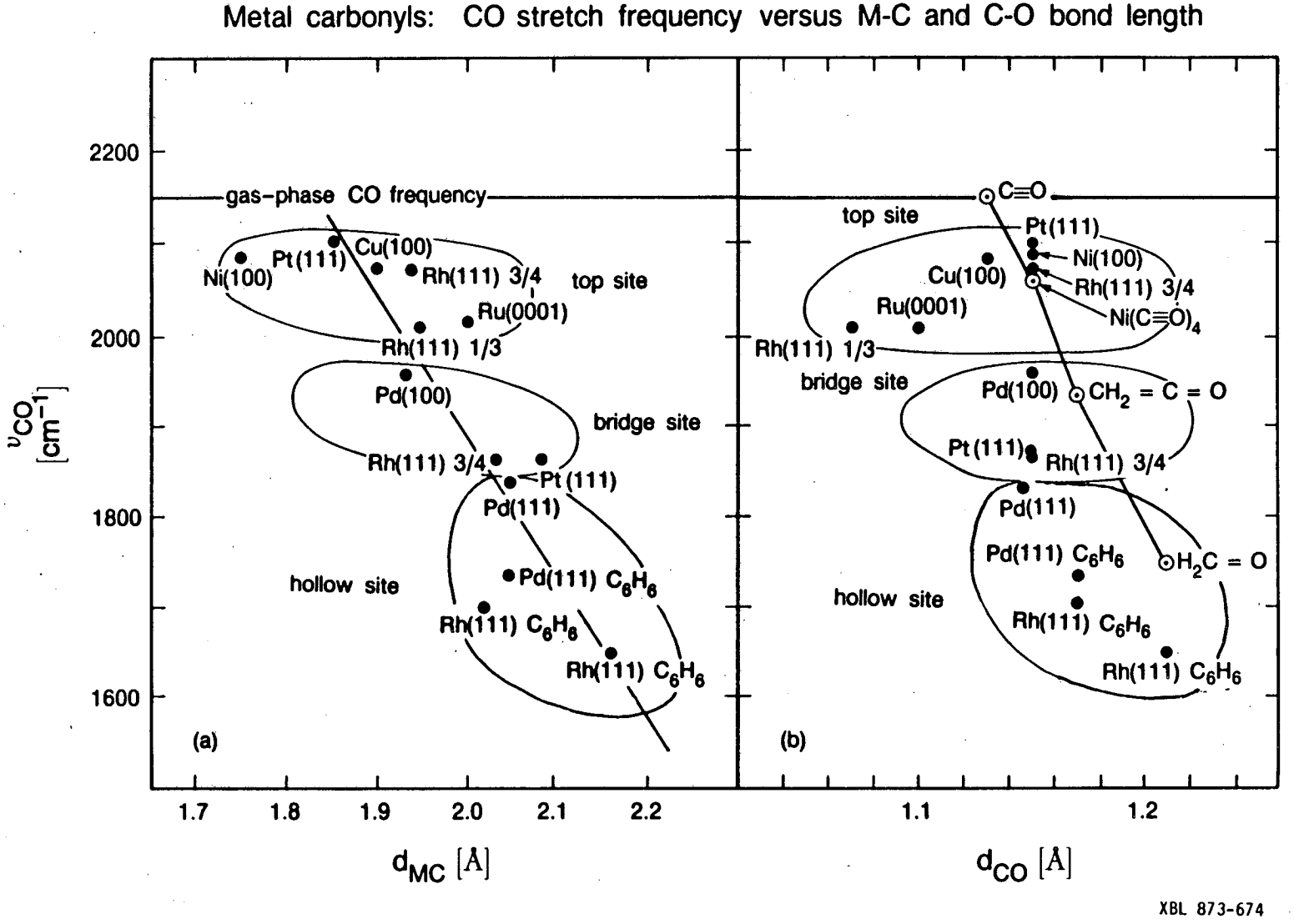
Metal carbonyls: CO stretch frequency versus M-C and C-O bond length
2200
2000
1800
1600
ν_{CO} [cm^{-1}]
gas-phase CO frequency
Ni(100)
Pt(111)
Cu(100)
Rh(111) 3/4
top site
Ru(0001)
Rh(111) 1/3
Pd(100)
bridge site
Rh(111) 3/4
Pt(111)
Pd(111)
hollow site
Pd(111) C_6H_6
Rh(111) C_6H_6
Rh(111) C_6H_6
(a)
1.7
1.8
1.9
2.0
2.1
2.2
d_{MC} [Å]
C≡O
top site
Pt(111)
Ni(100)
Cu(100)
Rh(111) 3/4
Ru(0001)
Ni(C≡O)$_4$
Rh(111) 1/3
bridge site
Pd(100)
$CH_2 = C = O$
Pt(111)
Rh(111) 3/4
Pd(111)
Pd(111) C_6H_6
$H_2C = O$
hollow site
Rh(111) C_6H_6
Rh(111) C_6H_6
(b)
1.1
1.2
d_{CO} [Å]
XBL 873-674

Fig. 7

LAWRENCE BERKELEY LABORATORY
TECHNICAL INFORMATION DEPARTMENT
UNIVERSITY OF CALIFORNIA
BERKELEY, CALIFORNIA 94720